Bull. Inst. Chem. Res., Kyoto Univ., Vol. 72, No. 2, 1994

X-ray Diffraction Study on Medium-Range Structure and Thermal Change of Silica Gel Made from Triethoxysilane by Sol-Gel Method

Kanichi KAMIYA*, Masanori WADA*, Masao IZUMI*,
Jun MATSUOKA* and Hiroyuki NASU*

Received May 25, 1994

Silica gel was prepared from triethoxysilane, $HSi(OC_2H_5)_3$ (HTES), by the sol-gel method. The medium-range (MR) structure was examined on the basis of the X-ray radial distribution analysis. It was found that a structure model deduced from hydrosilsesquioxane ladder polymer, $(HSiO_{1.5})_n$, which is composed of 4-fold siloxane rings (or tetra-cyclosiloxane), well simulated MR structure of the HTES-derived silica gel.

Thermal structure change of the gel in air was traced by the IR spectrometry and X-ray diffraction analysis. Above 300°C, ≡Si–H was oxidized to form ≡Si–OH, followed by the condensation between ≡Si–OH to form ≡Si–O–Si≡ bonds. At 300～500°C, the change of MR structure such as probably the reconstructive change of 4-fold siloxane rings to 6-fold ones, which was not so abrupt as the tetraethoxysilane (TEOS)-derived silica gel, was observed. The MR structure very similar to silica glass was not yet attained even at 1,000°C, while it was attained around 600°C in the case of the TEOS-derived silica gel.

KEY WODRS: Sol-Gel/ Triethoxysilane/ Medium-range structure/ X-ray diffraction/ IR spectra/ 4-fold siloxane ring(s)/ Ladder siloxane polymer(s)

1. INTRODUCTION

In the preparation of glasses through the sol-gel method, tetrafunctional alkoxysilanes (or silicon alkoxides), e.g. tetramethyl-ortho-silicate, $Si(OCH_3)_4$ (TMOS) and tetraethyl-ortho-silicate, $Si(OC_2H_5)_4$ (TEOS), have been widely used as sources of silica. The sol-gel reaction schema of these alkoxysilanes leading to silica gels and thermal conversion process of the gels to silica glass have been investigated by numerous authors using various techniques, and have been thoroughly and comprehensively reviewed by Sakka[1] and Brinker & Scherer.[2]

In addition to such tetrafunctional alkoxysilanes, di- or trifunctional alkoxysilanes such as monoalkyl (or phenyl)-tri-alkoxysilane (e.g. $CH_3Si(OR)_3$, $C_5H_6Si(OR)_3$, R=CH_3, C_2H_5, ...) and dialkyl-di-alkoxysilane (e.g. $(CH_3)_2Si(OR)_2$, $(C_2H_5)_2Si(OR)_2$, ...) have been attracting much attention as alternative starting materials for making inorganic-organic hybrid materials, so-called ORMOSIL (organically modified silicates), by the sol-gel method.[3] Furthermore, alkyl (or phenyl)-alkoxysilanes-derived silica gels lead to carbon-containing silica glass and/or silicon oxycarbide glasses when heat-treated in inert atmospheres.[4-13] When the $CH_3Si(OC_2H_5)_3$ (MTES)-derived silica gel was heat-treated in the flow of ammonia gas, the silica glass containing

* 神谷寛一, 和田正紀, 和泉正郎, 松岡 純, 那須弘行: Department of Chemistry for Materials, Faculty of Engineering, Mie University, Kamihama-cho, Tsu-shi, Mie-ken 514.

nitrogen (silicon oxynitride glass) was resulted.[14,15] There are published many papers devoted to reaction schema for the conversion process of these gels to oxycarbide and oxynitride glasses.[6~15]

Thus, nowadays, the sol-gel technology makes an important field in the glass-industry, and we can notice many sol-gel applications such as fiber-making, functional coating and optics.[16,17]

On the other hand, it is very recently that sol-gel investigators are interested in using trialkoxysilanes, $HSi(OR)_3$ as raw materials for silica glass. Pauthe et al.[18] prepared hydrophobic silica aerogel, in which $\equiv$Si–H bonds remain unattacked, from triethoxysilane, $HSi(OC_2H_5)_3$ (HTES). They also prepared silica gel from HTES and converted to the silicon oxynitride glass containing 6 wt% nitrogen by heat-treating in the flow of ammonia gas.[19]

As can be noticed by referring to many review papers and books, a plenty of information on the structure of hydrolysis products in the course of the sol-gel reaction of alkoxysilanes are available, and it is said that the sol-gel-derived silica glass has properties and structure essentially identical with melt-derived silica glass (except for defect structures and defect-dependent properties). However, to the present authors, it seems that the structural information, especially on the medium-range (MR) structure of the wet and/or dried gels is limited. The authors' queries are; whether the structure (e.g. 4-fold siloxane rings or tetra-cyclosiloxane) which is uncommon in the glass but characteristic of the siloxane oligomers formed in the course of hydrolysis of alkoxysilane is retained in the gel? and if so, how the structure of the oligomers does change to that of silica glass?

Standing on such queries, the present authors have been carrying out the neutron and X-ray diffraction study of the silica gels made from MTES and TEOS. The MTES-derived silica gel was well simulated with a methyl-silsesquioxane ladder polymer model consisting of 4-fold siloxane rings.[20] Furthermore, it was proposed on the basis of neutron and X-ray diffraction data that TEOS-derived silica gels are composed mostly of 4-fold siloxane rings,[21,22] and such a structure unit was considered to change by heat-treating at 400~600°C in air to the 6-fold siloxane ring which is a prevailing unit in the silica glass.

In the present work, the X-ray diffraction study was extended to the HTES-derived silica gel, and thermal evolution of the gel was examined by means of the IR spectrometry and X-ray diffraction. The results were compared with the TEOS-derived silica gel.

2. EXPERIMENTAL

2.1 Sample preparation

Triethoxysilane, $HSi(OC_2H_5)_3$ (HTES, Tokyo Chemicals Industry Co.) was used as a raw material. The solutions of which compositions are listed in Table 1 were prepared according to a flowchart shown in Fig. 1 (which is essentially the same as that used in the preparation of silica gels from TEOS). First, 0.06 mol of HTES was diluted with a half of prescribed amount of absolute ethanol in a 50 ml-tall beaker (~2 cm in diameter). Then, the mixture-solution of prescribed amount of distilled water, remaining half of absolute ethanol and HCl was added drop by drop to above ethanolic solution of HTES under stirred at ice/water temperature (0°C). The molar ratio of water to HTES was varied in the range 0.5~5.0, and that of HCl was kept constant at 0.001. The resultant clear $HTES/H_2O/C_2H_5OH/HCl$ solutions were warmed up to 60°C in open vessels to undergo hydrolysis and condensation reactions.

Table 1. Compositions and properties of HSi $(OC_2H_5)_3$ (HTES) solutions.

No.	HTES (g : mol)	Molar ratio			Sol	Gelation time
		HTES	H_2O	C_2H_5OH		
1	9.86 : 0.06	1	0.5	1.0	precipitation	—
2	9.86 : 0.06	1	1.0	1.0	clear	75 min
3	9.86 : 0.06	1	1.5	1.0	clear	25 min
4	9.86 : 0.06	1	1.5	5.0	clear	120 min
5	9.86 : 0.06	1	2.0	1.0	clear	20 min
6	9.86 : 0.06	1	3.0	1.0	clear	15 min
7	9.86 : 0.06	1	4.0	1.0	clear	12 min
8	9.86 : 0.06	1	5.0	1.0	clear	6 min

HCl/HTES=0.001 in all compositions.

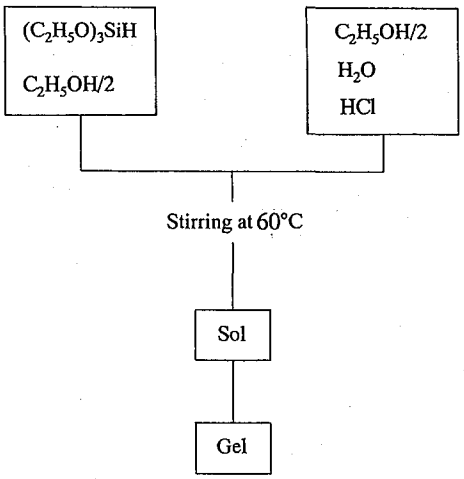

Fig. 1. Flowchart for the preparation of the silica gel from triethoxysilane (HTES).

While in solution 1 white precipitate was resulted, other solutions gave clear sols and set to transparent gels at times indicated in Table 1. Owing to high reactivity of HTES toward hydrolysis, the gelation time was very short compared to TEOS solutions.

Solution 7 with a molar ratio of water to TEOS of 4.0 was spread out on a polystyrene plate and set to gel. Gel films 10 to several tens μm in thickness were obtained.

Gel films thus prepared, and particulate gels made from solution 6 were heat-treated at various temperatures up to 1,000°C in air, and were subjected to infrared (IR) spectrometry and X-ray diffraction measurements.

2.2 Measurements

Infrared (IR) spectra of the gel film and heat-treated films were measured in the wavenumber range of 400 to 4,000 cm^{-1} with an IR spectrometer A202 (Nihon Bunko Co.).

DTA/TG analyses of the gel (No. 6) were carried out using a Rigaku TAS-100 type machine in air. A heating rate of 1 $K \cdot min^{-1}$ was adopted.

The ^{29}Si NMR spectrum of the gel was measured with JEOL-EX270 spectometer at 79.42 MHz using a spin rate of 5,000 Hz.

X-ray measurements were carried out using a Rigaku Geigerflex RAD type θ–θ X-ray diffractometer. The CuKα and MoKα radiations monochromatized by balanced filters and a graphite monochromator were used as X-ray sources. The scattering intensity was measured at intervals of 0.5° in the diffraction angle 2θ by a scintillation counter equipped with a pulse height analyzer, and up to at least 10,000 counts were accumulated at each angle. After correcting the intensities for polarization, absorption and back ground, the two scattering intensity curves obtained by using CuKα and MoKα radiations were combined to form a single curve. The maximum S $(=4\pi\sin\theta/\lambda)$ covered in the present work was 14.0 A^{-1}.

The corrected scattering intensities were normalized by the method combining Krogh-Moe & Norman's method with the high angle method, then were transformed into the atomic radial distribution function (RDF) by

$$\text{RDF}\ (r)=\sum_m K_m 4\pi r^2\rho_0+\frac{2r}{\pi}\int_0^{S_{\max}} S\cdot i(S)\cdot\exp(-\alpha^2S^2)\cdot\sin(S\cdot r)\cdot dS$$

where K_m is the effective number of electron in the specimen, r is the interatomic distance in A, $\exp(-\alpha^2S^2)$ is the damping factor, and

$$i(S)=\{I_{\text{obs}}-[\sum_m f_m{}^2+\sum_m(Z_m-\sum_j f_{mj}^2)]\}/f_e^2$$

in which $\sum_m(Z_m-\sum_j f_{mj}^2)$ is a term for Compton scattering and f_e is the average scattering factor of an electron.

The RDF curve was calculated for the structure model on the basis of the pair function method, in which a pair function, $P_{ij}(r)$, is correlated with observed RDF by

$$\sum_{uc}\sum_i\frac{N_{ij}}{r_{ij}}P_{ij}=\pi\text{RDF}/2\cdot r$$

where r_{ij} is the distance between atoms i and j, N_{ij} is the number of atom i around atom j in the unit chemical composition (uc). The function $P_{ij}(r)$ is evaluated from

$$P_{ij}(r)=\int_0^{S_{\max}}\frac{f_i f_j}{f_e^2}\cdot\exp(-\alpha^2S^2)\cdot\sin(S\cdot r_{ij})\cdot\sin(S\cdot r)\cdot dS$$

in which f_i and f_j are S-dependent atomic scattering factors of atoms i and j.

3. RESULTS

3.1 Structure of the HTES-derived silica gel

The IR spectrum and ^{29}Si NMR spectrum of the HTES-derived silica gel are shown in Fig. 2 and Fig. 3, respectively. IR absorption peaks at 450 cm^{-1} and 1,000~1,200 cm^{-1}, and a part of the peak around 850 cm^{-1} are assignable to the vibrations of Si–O bonds. An absorption band at 3,400~3,700 cm^{-1} is attributed to OH groups. A sharp peak at 2,250 cm^{-1} is due to Si–H bonds which also contribute to the peak around 880 cm^{-1}.[18] A small peak around 550 cm^{-1} will be concerned below. The over-all IR spectrum tells us that the HTES-derived silica gel is constructed with Si–O bonds and Si–H bonds remaining unreacted.

The ^{29}Si NMR spectrum consists of one strong peak accompanied with small peaks and/or shoulders. A strong peak at −85.5 ppm is due to tribranched silicate units, i.e., $O_3{\equiv}Si$–H named T_3.[23] Small peaks at −111~−112 ppm, −101.4 ppm and −77.3 ppm are ascribable

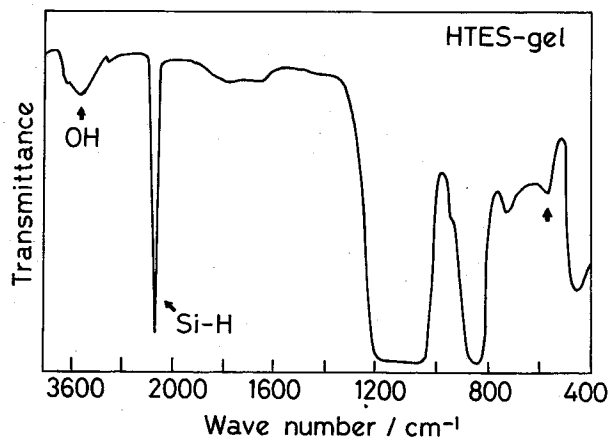

Fig. 2. IR spectrum of the HTES-derived-silica gel film.

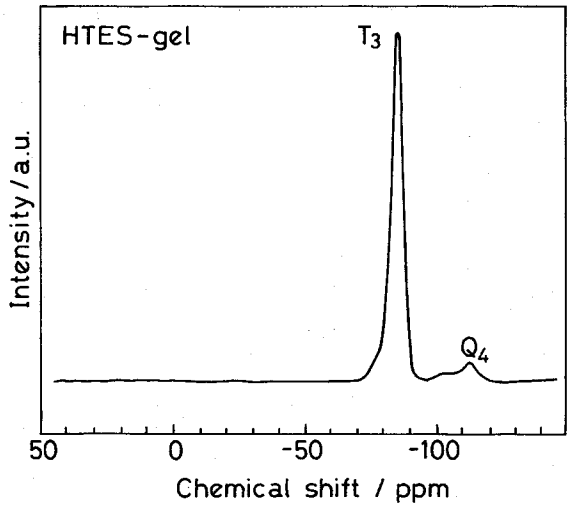

Fig. 3. ^{29}Si NMR spectrum of the HTES-derived-silica gel.

to SiO_4 (Q_4, i.e., Si in an SiO_4 tetrahedron in which all the oxygens are connected with the silicon atom), O_2=Si(OH)H and O_3≡Si–OH (Q_3) units, respectively.[23] Assuming the identical proportionality between the signal intensity and the content for each species, 90% or more of Si atoms in the gel is in T_3 units.

Eventually, the combination of the IR result and ^{29}Si NMR data may lead to the predominance of a structure unit of tetrahedral O_3≡Si–H (T_3) in the HTES-derived silica gel.

Figure 4 shows the X-ray scattering intensity curves of HTES-derived silica gel and melt-derived silica glass. The gel exhibits a marked small angle scattering, indicating that the gel is porous. In addition, the first sharp diffraction peak (at ~1.5 in S, FSDP) shifts toward high S value compared to silica glass as the TEOS-derived and MTES-derived silica gels do,[20-22] suggesting that the gel has a different medium-range (MR) structure from the silica glass.

The differential radial distribution function (d−RDF=RDF(r)−$\Sigma K_m 4\pi r^2 \rho$) curve of the HTES-gel and that of silica glass are shown in Fig. 5. The peaks appearing in the d-RDF curve

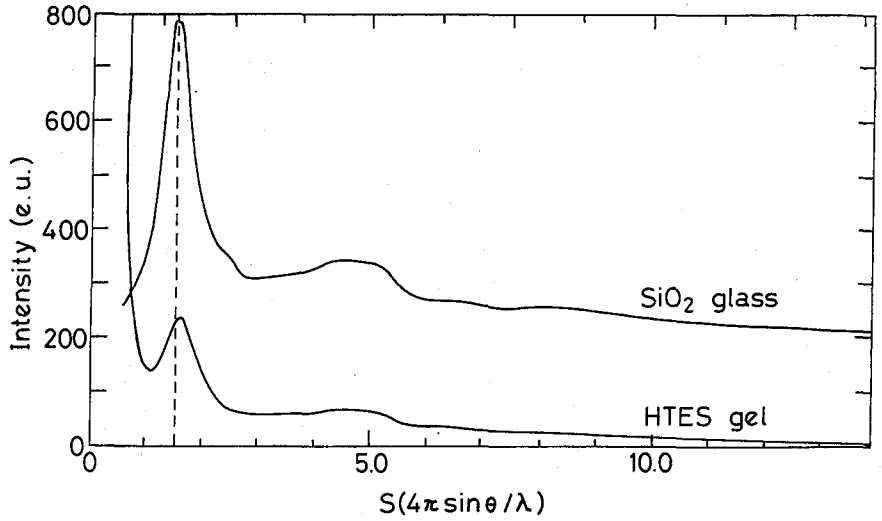

Fig. 4. X-ray scattering intensity curves of the HTES-derived silica gel and melt-derived silica glass.

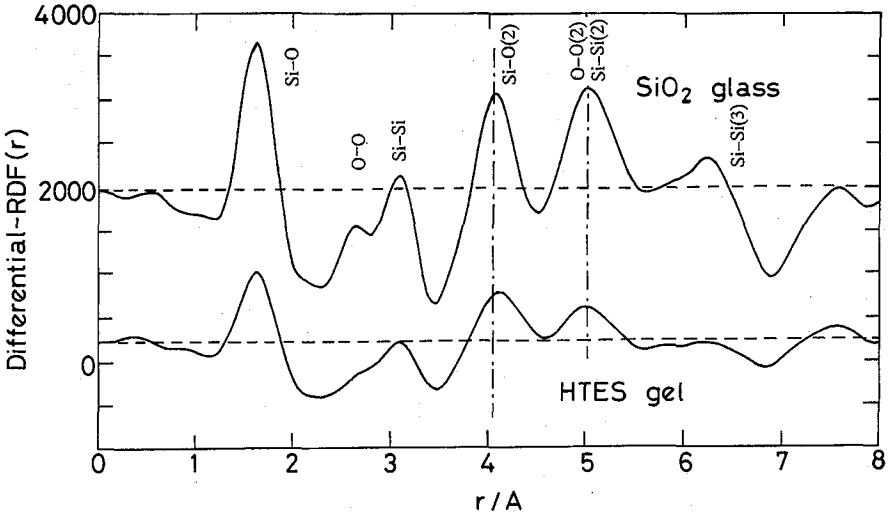

Fig. 5. Differential RDF curves of the HTES-derived silica gel and melt-derived silica glass.

of the silica glass which is composed mostly of 6-fold siloxane rings are assigned to respective interatomic distances indicated in the figure. All the peaks in *d*-RDF curve of the gel are smaller than those of the silica glass, which is attributed to the facts that the bulk density of the gel is smaller than that of silica glass and in the gel hydrogen atoms with a very small X-ray scattering factor replace a part of oxygens.

The position and peak height ratio for the peaks in *d*-RDF curve of the gel up to 3A are almost identical with those of the silica glass, implying that Si to 1st O, O to 1st O interatomic distances and intertetrahedral angle (evaluated from the Si to 1st Si distance) in the silica glass are almost retained in the gel. On the other hand, some differences in the peak position and

peak height ratio are observed above 3A between the gel and the silica glass. That is, the peak height ratio of a peak around 4A (4A-peak) to a peak around 5A (5A-peak) is larger than silica glass, and the separation between these two peaks is smaller than silica glass, which have been noted in the TEOS-derived silica gel,[22] also indicating the difference of MR structure of the gel or the linkage mode of tetrahedra from silica glass.

The simulation of RDF curve of the gel on the basis of the pair function method using a model structure was carried out for interpreting the MR structure. In modeling the gel structure, the $O_3{\equiv}Si{-}H$ tetrahedron should be the smallest structure unit as mentioned above. The tetrahedra could be linked with each others to form a network (or polymer) in different ways.

The small IR absorption band around 550 cm^{-1} in Fig. 2 may provide us with a clue for establishing the model structure of the HTES-derived silica gel. This IR band is observed in $R_2O{-}SiO_2$ (R=alkalis) glasses containing a relatively large amount of R_2O[24] and in the alkoxysilane-derived silica gels.[25,26] This band shows the prospery and decline pararrel to an absorption peak around 950 cm^{-1} due to $Si{-}O^-$ bonds. On the basis of this fact, the 550 cm^{-1} band has been assigned to $\equiv Si{-}O^-$ bending vibration.[24] In addition, this peak is observed in the silicate glasses and crystals which exhibit a relatively sharp Raman peak (so-called D_1) at about 490 cm^{-1},[27] suggesting some relation between the Raman D_1 and the IR 550 cm^{-1} band.

The explanation or assignment of Raman D_1 peak is controversial. Many investigators stand on the Galeener's result[28] which states that D_1 peak is due to 4-fold siloxane rings in the glasses. In contrast, several authors relate D_1 peak to $\equiv Si{-}O^-$ bending vibration based on the experimentally observed linear relationship between Raman D_1 peak and the 950 cm^{-1} peak due to $\equiv Si{-}OH$ stretching vibration,[29-31] which may suggest that the IR 550 cm^{-1} band is also related to $\equiv Si{-}OH$ bonds.[32]

However, there are several experimental facts which would support close relation of Raman D_1 peak and IR 550 cm^{-1} band to 4-fold siloxane rings: ① Coesite crystal which is composed of interconnected 4-fold siloxane rings and has no non-bridging oxygens gives a sharp and strong Raman peak at 510 cm^{-1},[33] and IR absorption peaks at 500~600 cm^{-1}. Anorthite and orthoclase crystal which also contain 4-fold siloxane rings (a part of Si is replaced by Al) and no $\equiv Si{-}O^-$ bonds show a Raman peak at 503 and 513 cm^{-1}, respectively[34] and IR band around 550 cm^{-1}.[25] ② Some cyclic siloxane tetrameters (4-fold siloxane rings), $[X_2SiO]_4$, where X=H, CH_3, C_2H_5, C_5H_6 ...) give a small IR band in the range 510~600 cm^{-1}.[35,36] In these cases, if $\equiv Si{-}X$ bending vibration is concerned, the absorption peak would appear at much different frequencies depending on the species X.

Accordingly, it may be reasonable to consider that the HTES-derived silica gel involves 4-fold siloxane ring units.

Next problem is how to connect the 4-fold siloxane rings with each others to form a network. It has been known that $XSi(OR)_3$ (X=H, CH_3, C_2H_5, C_5H_6 ...) produces various kinds of siloxane oligomers on hydrolysis.[37,38] Roughly speaking, the oligomers are classified into two categories. The ladder polymers consisting of 4-fold siloxane rings belong to one category, and polyhedral oligomers formed by intramolecular cyclization of 4-fold siloxane rings or ladder type oligomers belong to the other. For simplicity, we started with two simplest oligomers; octa (hydrosilsesquioxane), T_8 and a linear ladder oligomer shown in Fig. 6a and b. In T_8 model, only T_3 ($O_3{\equiv}Si{-}H$) units are there, and in the ladder type model T_3 units are prevailing and a fraction of $O_2{=}Si(OH)H$ (Q_2) is at the terminals.

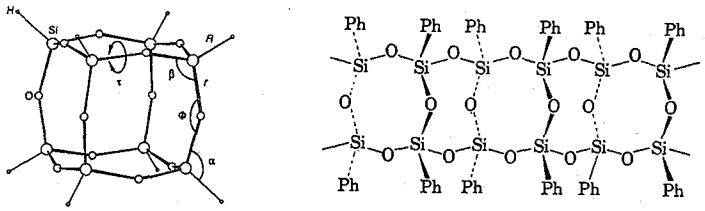

(a) (b)

Fig. 6. Illustration of (a) octa (hydrosilsesquioxane), T_8, and (b) ladder polysilsesquioxane.[40]

The similarity of the corresponding interatomic distances in these two models in the range up to ~6A[39,40] makes it difficult to determine the superiority of one model over the other until the connection of respective model units to form a polymer or network is taken into consideration. For T_8 model, at least two corners have to be bonded through ≡Si–O–Si≡ bonds in order to form a network, changing the silicon environment at corners from T_3 to Q_4 and the fraction of Q_4 of 2/8=25% being resulted. This fraction of Q_4 is too large to elucidate the ^{29}Si NMR result of the present silica gel (Fig. 3). On the contrary, ladder siloxane oligomers can be polymerized through the condensation reaction between $=O_2Si(H)$–OH attached to the terminals, increasing Q_3 units more and more at the expense of Q_2 as illustrated in Fig. 7. In this case, ideally, no Q_4 environment should be resulted on the formation of polymers or the network. If a part of ≡Si–H bonds in the oligomer happens to have been changed to ≡Si–OH in the course of sol-gel reaction of HTES, Q_4 environment may be formed in the polymerization through the condensation between ≡Si–OH. This polymerization scheme of ladder siloxane oligomers can explain very small contents of Q_2 and Q_4 species in the gel.

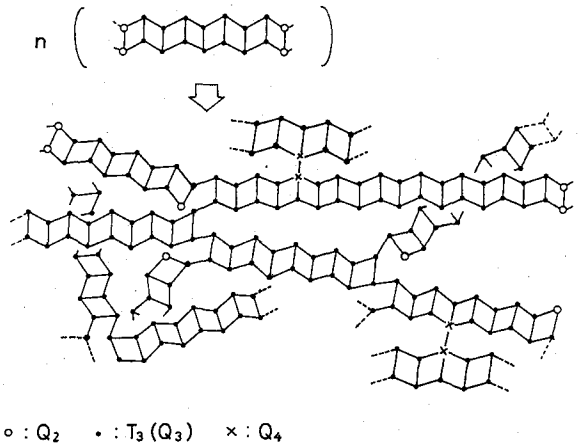

Fig. 7. Schematic presentation of the connection of ladder silsesquioxane oligomers to form a network, ○: Q_2, ●: T_3, ×: Q_4.

Consequently, it seems that the ladder siloxane prefers to T_8 as a structure model of the HTES-derived silica gel. Another thing to be mentioned is that the gel has been made in the present work from HTES under such a hydrolysis condition that makes the formation of

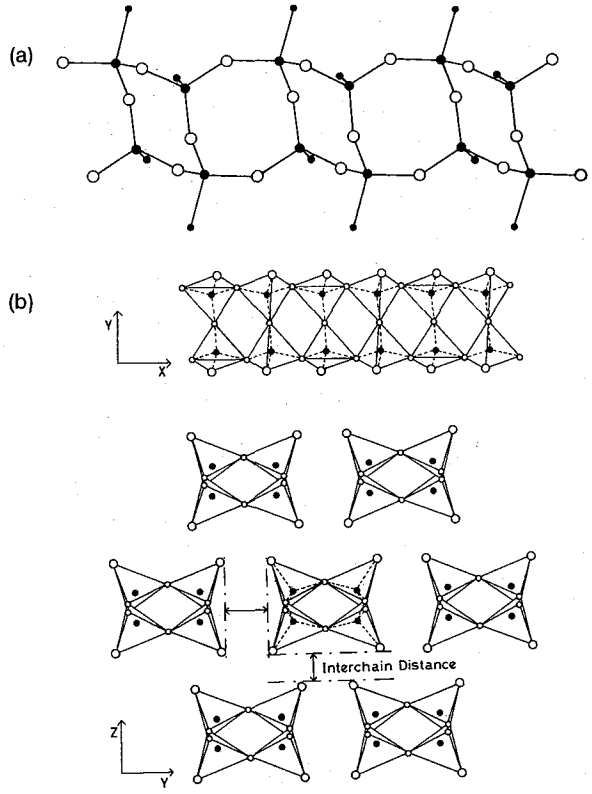

Fig. 8. Structure units for the HTES-silica gel. (a) model unit consisting of 4-fold siloxane rings, (b) spacial arrangement of the model units.

Table 2. Average structure parameters of ladder type silsesquioxane model for HTES gel.

O–Si–O angle/degree	Si–O–Si angle/degree	Si–O distance/A	Si–H distance/A	Interchain distance/A
112.0	147.0	1.62	1.46	2.0～2.5

polyhedral siloxanes (or cage-like siloxanes) more difficult than the ladder type siloxanes[37,41,42].

The schematic structure model unit and its spacial arrangement (Fig. 8) were made up by referring to the structure of phenylsilsesquioxane ladder polymer (Fig. 6b[40]) and MTES-derived silica gel.[20]

The RDF/r curve calculated using this model having structure parameters given in Table 2 is shown in Fig. 9 by a solid line, together with observed RDF/r (dotted line). It can be seen that there is only a slight difference between observed and calculated RDF/r curves up to 3A, and that the peaks in calculated curve above 3A are sited at r values similar to those in observed one. So, then, the structure disorder which increases in proportion to r was introduced into the model as a statistical distribution of each pair function $P_{ij}(r)$.

The final result is shown in Fig. 10, in which a very good fit of the calculated RDF/r with the observed one is noted in the r range up to 6A.

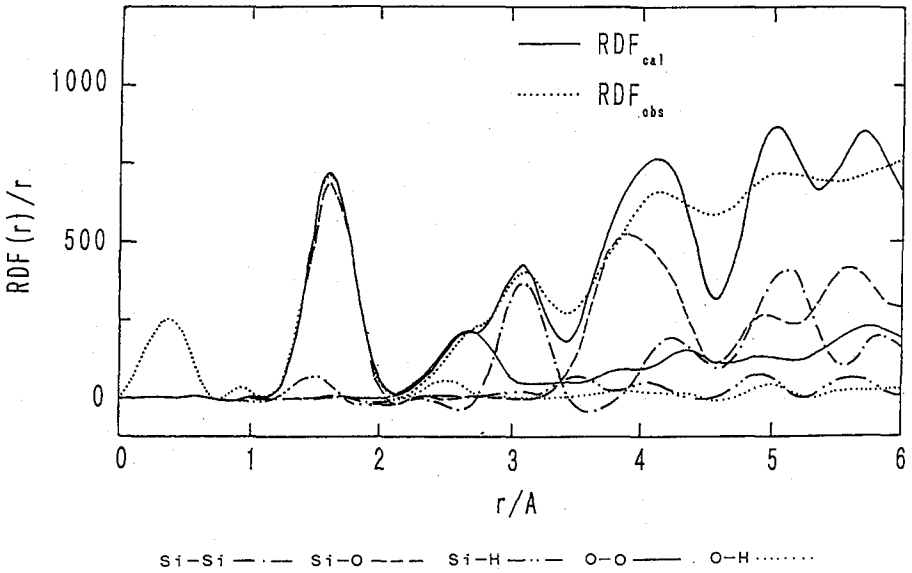

Fig. 9. X-ray radial distribution function (RDF/r) curve of the HTES-derived silica gel, ---; observed, ——; calculated.

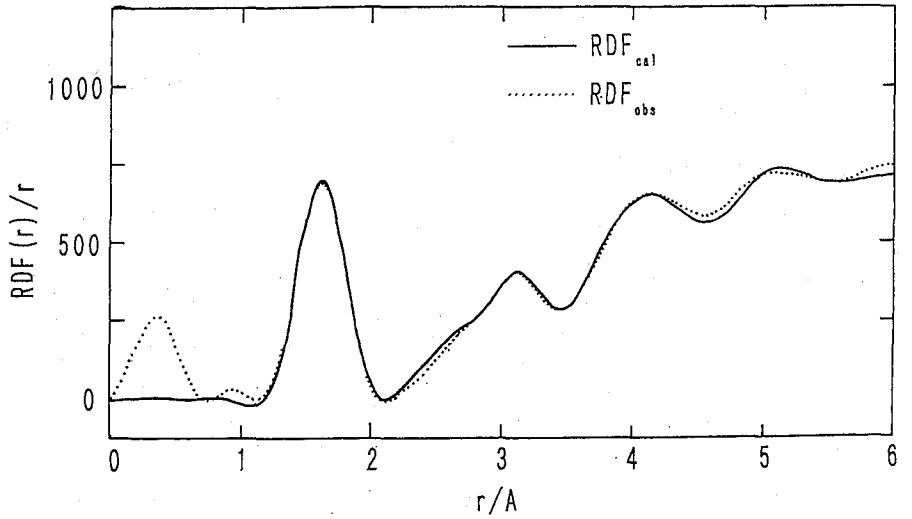

Fig. 10. Calculated RDF/r of the HTES-derived silica gel (——), after introduction of structure disorder.

3.2 Thermal evolution of the gel

In Fig. 11, IR spectra of the HTES-derived silica gel films heat-treated at indicated temperatures are shown. The absorption coefficient of respective IR peaks except for the saturated one around 1,100 cm^{-1} is plotted against the heat-treatment temperature in Fig. 12. As can be seen from these two figures, no important change of the spectrum or absorption coefficients of all the peaks but ~3,500 cm^{-1} band due to OH groups is not observed up to 250°C.

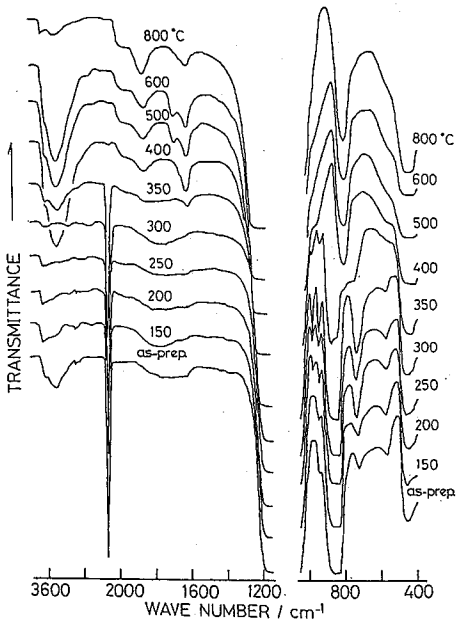

Fig. 11. IR spectra of the HTES-derived silica gel films heat-treated at various temperatures.

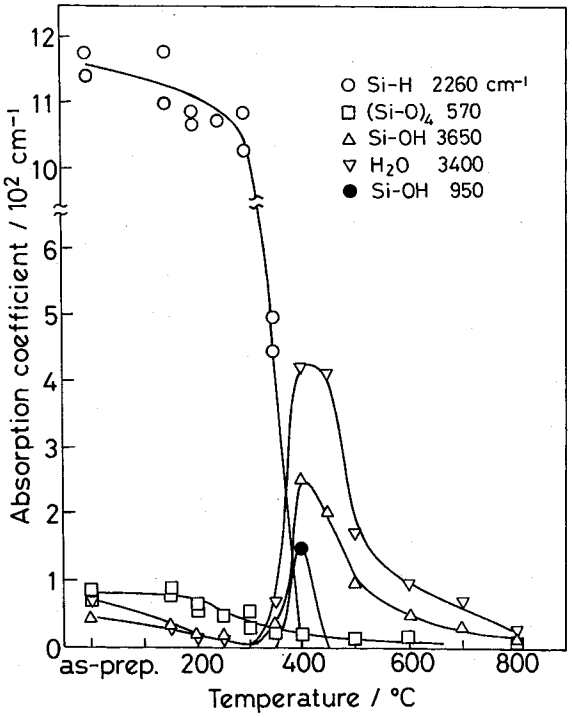

Fig. 12. The change of absorption coefficients of the respective chemical bond species with heat-treatment temperature for the HTES-derived silica gel films.

A drastic change in IR spectrum is observed in the narrow temperature range of 300~400°C, where the peak due to Si-H (at 2,250 cm^{-1}) abruptly disappears and, instead, the peak due to OH (~3,500 cm^{-1}) develops rapidly, followed by the gradual decrease. The ~550

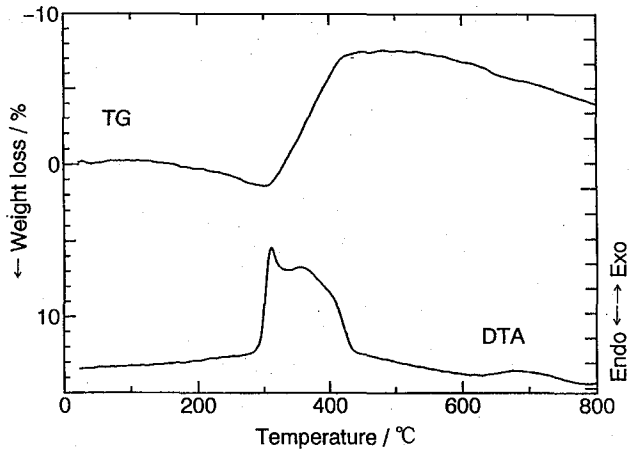

Fig. 13. TG/DTA curves of the HTES-derived silica gel in air.

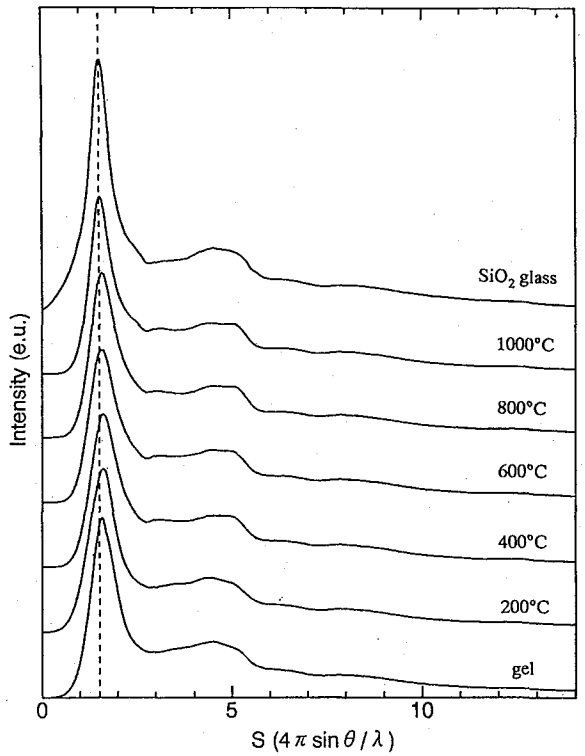

Fig. 14. X-ray scattering intensity curves of the HTES-derived silica gels heat-treated at various temperatures.

cm^{-1} band which is ascribable to 4-fold siloxane rings starts to decrease at 300°C, but is still present at 800°C. These facts indicate that the decrease of Si–H bonds is closely related to the formation of Si–OH bonds, and the decrease of 4-fold siloxane rings is associated with the decrease of Si–H and/or Si–OH bonds.

Figure 13 shows TG and DTA curves of the HTES-derived silica gel (made from solution 6). The gel exhibits once a slight decrease of weight up to about 300°C, and then a drastic increase of weight in the heat-treatment temperature range of 300～400°C. A slight decrease in weight up to 200～300°C may be attributed to the removal of H_2O bonded to H in Si–H through the hydrogen bonding.[18] The temperature range where the steep increment of weight occurs corresponds to that for the drastic change of IR spectrum, in other words, weight change may be associated with the prosperity and decline of Si–H and Si–OH bonds.

The change of X-ray scattering intensity curve of the HTES-derived silica gel with the heat-treatment temperature is shown in Fig. 14. The corresponding differential radial distribution function (*d*-RDF) curves are shown in Fig. 15. Both the scattering curve and *d*-RDF curve of the gel become more and more similar to those of silica glass as the heat-treatment temperature is raised, as in the case of the TEOS-derived silica gel.[22] In particular, the peak height ratio of 4A-peak to 5A-peak in *d*-RDF curve is decreased with increasing heat-treatment temperature. Other two parameters characterizing the silica gel, i.e., the position of FSDP in the X-ray scattering intensity curve and the peak to peak separation between 4A and 5A-peaks are shown as

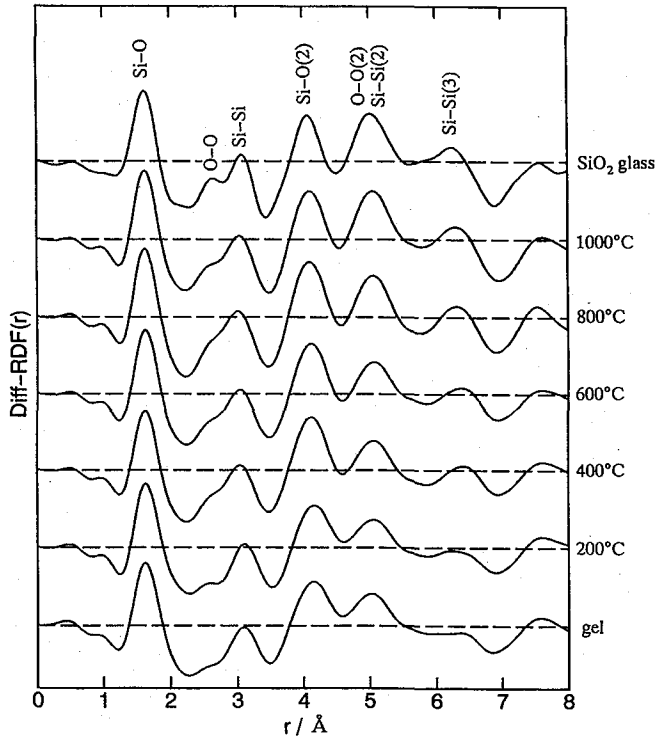

Fig. 15. Differential RDF curves of the HTES-derived sillica gels heat-treated at various temperatures.

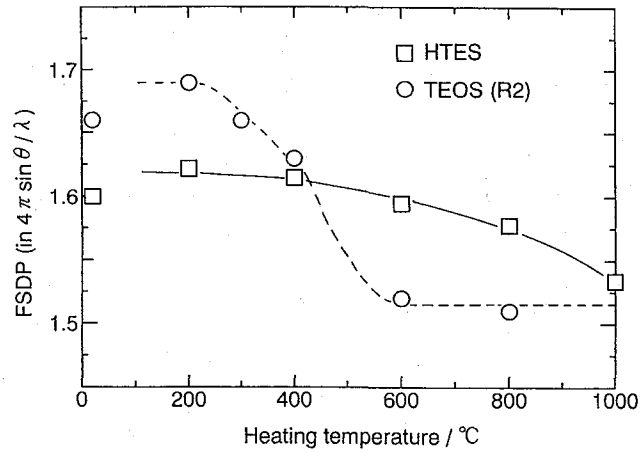

Fig. 16. Change of FSDP position in X-ray scattering intensity curve with heat-treatment temperature. –□–; HTES-silica gel, –○–; TEOS-silica gel.

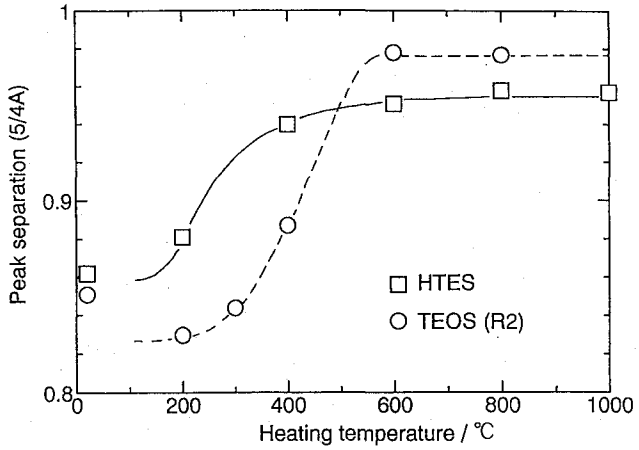

Fig. 17. Peak separation between 4A and 5A peaks in the RDF curve as a function of heat-treatment temperature. –□–; HTES-silica gel, –○–; TEOS-silica gel.

a function of temperature in Fig. 16 and Fig. 17.

The FSDP shifts gradually toward the position of the silica glass with the increase of heat-treatment temperature. On the other hand, the peak separation increases abruptly at 200～400°C, where the occurrence of a remarkable structure change has been pointed out from IR and TG/DTA data. The heat-treatment temperature dependence of FSDP and/or the peak separation in *d*-RDF is rather smaller for the HTES-gel than the TEOS-gel. Despite of such a difference, as a whole, the 4-fold siloxane rings in the HTES-gel are considered to change by the heat-treatment to that of the silica glass, i.e., 6-fold siloxane rings. However, it should be noted that the FSDP and peak separation in *d*-RDF of the HTES-gel are still deviated slightly from those of silica glass even at 800～1,000°C, indicating that the conversion of the gel to glass is not yet complete.

4. DISCUSUSSION

The ladder siloxane polymer model was found to prefer to T_8-model for interpreting MR structure of the HTES-derived silica gel. However, the possibility of using polyhedral siloxanes, T_n, with n larger than 8 as structure models has not been completely abandoned. These species would be produced by the hydrolysis of HTES, as well as ladder type polysiloxanes[37,38]. When those polyhedral siloxanes are connected with each others at two corners to form a network, the fraction of the resultant Q_4 species decreases from 25% for T_8 with the increase of n, the fraction of $Q_4 < 10\%$ being encountered for T_n ($n > 20$). However, in such a large polyhedral cage-like siloxanes, the MR structure may become similar to that in the ladder type siloxanes. Furthermore, the description of the gel structure as the ladder type siloxane is so simplified, and the polyhedral cage-like siloxane with a ladder type siloxane as a side group would still remain as one of the candidates for the structure model of HTES-derived silica gel.

The ladder siloxane model which could simulate well the HTES-derived silica gel is very similar to that of the MTES-derived silica gel, which as a matter of course interprets the shift of FSDP toward high S, and provides higher peak height ratio of 4A-peak to 5A-peak in d-RDF curve or more compact MR structure than melt-derived silica glass.

As has been reported,[22,43-46] the feature of the X-ray scattering intensity curve of the TEOS-derived silica gel and corresponding d-RDF is also very similar to those of the HTES-gel. Namely, the shift of FSDP toward high S value and high peak height ratio of the 4A-peak to the 5A-peak compared to silica glass are observable. Himmel et al.[45,46] explained such X-ray data using primary particles composed of eight puckered 6-fold siloxane rings (as those in the low-quartz). On the other hand, the present authors elucidated, in rather a semiquantitative way, X-ray data of the TEOS-gel in terms of 4-fold siloxane rings by referring to Yamana's results[47] on the silica glass heat-treated under high pressure. The result obtained in the present work may confirm our structure assumption made for the TEOS-derived silica gel. The ^{29}Si NMR data which indicate that Q_3 species are predominant in the silica gel made from TEOS[48] are also consistent with the ladder type siloxane model consisting of 4-fold siloxane rings.

As is seen in Fig. 15 and Fig. 16, the FSDP position and the peak separation between 4A and 5A-peaks are slightly different from the TEOS-derived silica gel, which may be caused by the difference in chemical species terminating 4-fold siloxane rings (≡Si–H in the HTES-gel and probably ≡Si–OH in the TEOS-gel).

Thermal evolution of the HTES-derived silica gel has been examined by several authors by means of TG/DTA analyses combined with gas chromatography and IR spectrometry. Belot et al.[49] prepared the silica gel consisting of O_3≡Si–H units from HTES through the hydrolysis under the acidic condition and pursued the thermal change under the argon atmosphere. They found that the gel was slightly decomposed to SiH_4 and H_2 above 300°C (weight decrease of about 3% was resulted). Pauthe's HTES-silica gel prepared under the neutral condition exhibited about 10% weight gain at 300~500°C in air, which suggested the occurrence of oxidation of ≡Si–H to ≡Si–OH which was followed by the condensation reaction to ≡Si–O–Si≡ network.[18]

The TG curve of the gel made in the present work is very similar to Pauthe's. A very sharp exothermic peak around 300°C and successive somewhat broadened peak centered around 350°C in DTA curve indicate that the oxidation of ≡Si–H to ≡Si–OH occurs very abruptly and formed

≡Si–OH are less abruptly condensated to ≡Si–O–Si≡ network.

The Si–H bonds are scarcely observed in the present gel above 400°C, while in Pauthe's gel Si–H species is still discernible at 600°C. The retention of this species at such a high temperature in the latter case may be due to the bulkiness of the gel specimen. The gradual decrease of weight with the increase of the heat-treatment temperature above 500°C both in Pauthe's gel and present gel may imply that the condensation reaction of Si–OH to form the siloxane network is continued up to higher temperatures as is suggested from IR spectrometry data.

The difference of thermal evolution behavior of the HTES-silica gel from the TEOS-silica gel is noticed in the heat-treatment temperature dependence of the FSDP position and the peak separation between 4A and 5A-peaks in d-RDF curve. Apart from the facts that these two parameters of the HTES-gel are nearer those of silica glass than the TEOS-gel, the change of the parameters of the HTES-gel on heating is rather gradual than the TEOS-gel, and do not reach the values for silica glass even at 1,000°C. Such a difference is considered to be related to the content of remaining OH groups. As is evaluated from the absorption coefficient of OH around 3,500 cm^{-1} (Fig. 12), the content of OH is as high as a few wt% even at 800°C, being much larger than the 800°C-treated TEOS-gel in which the 3,500 cm^{-1} peak is scarcely observed (Figs. 3 and 4 in ref. 25). It is considered that the remaining OH plays an important role for stabilizing 4-fold siloxane rings as other O_3≡Si–X (X : H, CH_3, C_5H_6 ...) do, leading to still a different MR structure from the melt-derived silica glass and the TEOS-derived silica gel heat-treated at 1,000°C. In some cases, highly porous nature of the alkoxy-derived silica gel has been ascribed to the retention of such a high content of OH groups in the heated mass,[50] because Si–OH groups on the surface of big pores are too much separated to be condensated among themselves.

5. CONCLUSION

The silica gel was prepared from triethoxysilane, $HSi(OC_2H_5)_3$ (HTES) by the sol-gel method. The medium-range (MR) structure of the gel was examined by the X-ray diffraction technique on the basis of the pair function analysis, and thermal evolution of the gel was examined and compared with the silica gel made from tetraethoxysilane, $Si(OC_2H_5)_4$ (TEOS). Following results were obtained.

(1) The slow hydrolysis of triethoxysilane at 60°C under the acidic condition led to the clear and transparent gel within several ten minutes, depending on the amount of added water.

(2) The structure model deduced from hydrosilsesquioxane ladder polymer $(HSiO_{1.5})_n$, which is composed of 4-fold siloxane rings, well simulated MR structure of the HTES-derived silica gel.

(3) The structure model for the HTES-silica gel was very similar to that for the monomethyl-tri-ethoxysilane (MTES)-derived silica gel. And it was considered from the close comparison of the X-ray scattering intensity curve and differential radial distribution curve between the HTES-gel and the TEOS-gel that this ladder siloxane type model is also applicable to the TEOS-derived silica gel.

(4) On heat-treating in air, Si–H bonds in the HTES-gel was oxidized in the temperature range of 300~500°C, followed by the condensation of formed Si–OH bonds to ≡Si–O–Si≡ network. A drastic change of MR change, i.e., the reconstructive change of 4-fold siloxane rings

to 6-fold siloxane rings was observed in this heat-treatment temperature range.

(5) The thermal change of MR structure of the HTES-gel was more gradual than the TEOS-gel with respect to the heat-treatment temperature. The retention of a small amount of 4-fold siloxane rings above 800°C was attributed to a relatively large fraction (a few wt%) of Si–OH remaining uncondensated.

REFERENCES

(1) S. Sakka, in : "Treatise on Materials Science and Technology", Vol. 22, eds. M. Tomozawa and R. Doremus, Academic Press, New York, pp. 129–167 (1982) ; S. Sakka, "Zoru-Geru-Ho no Kagaku" (in Japanese), Agune-Shofu-Sha, Tokyo (1988).

(2) C.J. Brinker and G.W. Scherer, "Sol-Gel Science", Academic Press Inc., Boston (1990).

(3) H. Schmidt, New Type of non-crystalline solids between inorganic and organic materials, *J. Non-Crystalline Solids,* **73**, 681–691 (1985).

(4) F.K. Chi, Carbon-containing monolithic glasses via sol/gel process, *Ceram. Eng. Sci., Proc.,* **4**, 704–717 (1983).

(5) K. Kamiya, T. Yoko, T. Sano and K. Tanaka, Distribution of carbon particles in carbon/SiO_2 glass composites made from $CH_3Si(OC_2H_5)_3$ by the sol-gel method, *J. Non-Crystalline solids,* **119**, 14–20 (1990).

(6) K. Kamiya, T. Yoko, K. Tanaka and M. Takeuchi, Thermal evolution of gels derived from $CH_3Si(OC_2H_5)_3$ by the sol-gel method, *J. Non-Crystalline Solids,* **121**, 182–187 (1990).

(7) H. Zhang and C.G. Pantano, Synthesis and characterization of silicon oxycarbide glasses, *J. Am. Ceram. Soc.,* **73**, 958–963 (1990) ; H. Zhang and C.G. Pantano, High temperature stability of oxycarbide glasses, *Mat. Res. Soc. Symp. Proc.,* **271**, 783–788 (1992).

(8) K.C. Chen, K.J. Thorne, A. Chemseddine, F. Babonneau and J.D. Mackenzie, Silicon carbide via the hydrolysis-condensation process of dimethyldiethoxysilane/tetraethoxysilane copolymers, *Mat. Res. Soc. Symp. Proc.,* **121**, 57–574, (1988) ; F. Babonneau, L. Bois and J. Livage, Silicon oxycarbides via sol-gel route ; characterization of the pyrolysis process, *J. Non-Crystalline Solids,* **147** & **148**, 280–284 (1992).

(9) F. Babonneau and L. Bois, Sol-gel synthesis of a siloxypolycarbosilane gel and its pyrolytic conversion to silicon oxycarbide, *Chem. Mater.* **6**, 51–57 (1994).

(10) G.M. Renlund, S. Prochazka and R.H. Doremus, Silicon oxycarbide glasses : Part I, Preparation and chemistry, *J. Mat. Res.,* **6**, 2716–2722 (1991) ; G.M. Renlund, S. Prochazka and R.H. Doremus, Silicon oxycarbide glasses : Part II, Structure and properties, *J. Mat. Res.,* **6**, 2723–2734 (1991).

(11) V. Raman, O.P. Bahl and N.K. Jha, Synthesis of silicon oxycarbide through the sol-gel process, *J. Mat. Sci., Letters,* **12**, 1188–1190 (1993).

(12) A. Katayama, K. Kamiya, H. Nasu and J. Matsuoka, Structure and property of carbon-containing silica glass fibers made by the sol-gel method (in Japanese), Preprints of the 1993 Annual Meeting of Japan Ceramic Society, Tokyo, p. 170 (1993) ; K. Kamiya, A. Katayama, H. Nasu and J. Matsuoka, Preparation of oxycarbide glass fibers by the sol-gel method (in Japanese), *New Glass,* **9**, 4–15 (1994).

(13) V. Belot, R.J.P. Corrin, D. Leclercq, P.H. Mutin and A. Vioux, Thermal reactions occurring during pyrolysis of cross linked polysilane gels, precursor to silicon oxycarbide glasses, *J. Non-Crystalline Solids,* **147** & **148**, 52–55 (1992).

(14) K. Kamiya, M. Ohya and T. Yoko, Nitrogen-containing SiO_2 glass fibers prepared by ammonolysis of gels made from silicon alkoxides, *J. Non-Crystalline Solids,* **83**, 208–222 (1986).

(15) H. Unuma, M. Yamamoto, Y. Sukuki and S. Sakka, *J. Non-Crystalline Solids,* **128**, 223–230 (1991).

(16) L.C. Klein (ed.), "Sol-gel technology for thin films, fibers, performs, electronics and specialty shapes", Neyes Publishers, Park Ridge, N.J. (1988).

(17) L.C. Klein (ed.), Sol-gel optics : "Processing and applications", Kluwer Academic Publishers, Boston (1994).

(18) M. Pauthe, F. Despetis and J. Phalippou, Hydrophobic silica CO_2 aerogels, *J. Non-Crystalline Solids,* **155**, 110–114 (1993).

(19) M. Pauthe, J. Phalippou, V. Belot, R. Corriu, D. Leclercq and A. Vioux, Preparation of oxynitride silicon glasses I. Nitridation of hydrogeno-silsesquioxane xerogels, *J. Non-Crystalline Solids,* **125**, 187–194 (1990).

(20) M. Wada, K. Kamiya and H. Nasu, X-ray diffraction analysis of SiO_2 gel prepared from monomethyl-

tri-ethoxysilane by the sol-gel method, *Phys. Chem. Glasses,* **33**, 56–60 (1992).
(21) M. Wada, K. Kamiya, H. Nasu, J. Matsuoka, T. Yoko, T. Fukunaga and M. Misawa, Structure analysis of sol-gel-derived SiO_2 gels by neutron diffraction, *J. Non-Crystalline Solids,* **149**, 203–208 (1992).
(22) K. Kamiya, M. Wada, J. Matsuoka, H. Nasu, T. Fukunaga and M. Misawa, Diffraction study of the sol-gel-derived SiO_2 gels, Proc. XVI, Intern. Cong. Glass, Vol. 7, pp. 33–38 (1992).
(23) V. Belot, R.J.P. Corriu, D. Leclercq, P.H. Mutin and A. Vioux, Thermal redistribution reactions in cross linked polysilanes, *J. Polymer Sci., Part A, Polymer Chem.,* **30**, 613–623 (1992).
(24) H. Toyuki, Effect of Na_2O on the nature of Si-O bonds in Na_2O-SiO_2 glasses (in Japanese), *Yogyo-Kyokai-Shi,* **85**, 554–558 (1977).
(25) H. Yoshino, K. Kamiya and H. Nasu, IR study on the structural evolution of sol-gel-derived SiO_2 gels in the early stage of conversion to glasses, *J. Non-Crystalline Solids,* **126**, 68–78 (1990).
(26) D.L. Wood and E.M. Rabinovich, Study of alkoxide silica gel by infrared spectroscopy, *Appl. Spectrosc.* **43**, 263–267 (1989).
(27) B.C. Bunker, D.R. Tallant, T.J. Headley, G.L. Turner and R.J. Kirkpatrick, *Phys. Chem. Glasses,* **29**, 106 (1988).
(28) F.L. Galeener, R.A. Barrio, E. Martinez and R.J. Elliot, *Phys. Rev. Lett.* **53**, 2429 (1984).
(29) A. Chmel, E.K. Mazurina and V.S. Shashkin, Vibrational spectra and defect structure of silica prepared by non-organic sol-gel process, *J. Non-Crystalline Solids,* **122**, 285–290 (1990).
(30) B. Humbert, A. Burneau, J.P. Gallas and J.C. Lavalley, Origin of Raman bands D_1 and D_2 in high surface area and vitreous silicas, *J. Non-Crystalline Solids,* **143**, 475–483 (1992).
(31) C.A.M. Mulder and A.A.J.M. Damen, The origin of the "defect" 490 cm^{-1} Raman peak in silica gel, *J. Non-Crystalline Solids,* **93**, 387–394 (1987).
(32) M.C. Matos, L.M. Ilharco and R.M. Almeida, The evolution of TEOS to silica gel and glass by vibrational spectroscopy, *J. Non-Crystalline Solids,* **147&148**, 232–237 (1992).
(33) R. Hemley, H. Mao, P. Bell and B. Mysen, Raman spectroscopy of SiO_2 glass at high pressure, *Phys. Rev. Letters,* **57**, 747 (1986).
(34) S.K. Sharma, J.A. Philpotts and D.W. Matson, Ring distributions in alkali and alkaline earth aluminosilicate framework glasses—A Raman spectroscopic study, *J. Non-Crystalline Solids,* **71**, 403–410 (1985).
(35) A.L. Smith and D.R. Anderson, Vibrational spectra of Me_2SiCl_2, Me_3SiCl, $Me_3SiOSiMe_3$, $(Me_2SiO)_3$, $(Me_2SiO)_4$, $(Me_2SiO)_x$ and their deuterated analogs, *Appl. Spectrosc.*, **38**, 822–834 (1984).
(36) O.K. Johanson and C-L. Lee, in "Cyclic Monomers", ed. K.C. Frisch, Wiley, New York, p. 459 (1971).
(37) M.G. Voronkov and V.L. Lavrentyev, Polyhedral oligosilsesquioxanes, in "Topics in Current Chemistry", **102**, 199–236 (1982).
(38) C.L. Frye and W.T. Collins, The oligomeric silsesquioxane, $(HSiO_{1.5})_n$, *J. Am. Chem. Soc.,* **92**, 5586–5588 (1970).
(39) G. Calzaferri and R. Hoffman, The symmetrical octasilasesquioxanes $X_8Si_8O_{12}$: Electronic structure and reactivity, *J. Chem. Soc. Dalton Trans.*, 917–928 (1991).
(40) J.F. Brown Jr., L.H. Vogt Jr., A. Katchman, J.W. Eustance, K.M. Kiser and K.W. Krantz, Double chainpolymers of phenylsilsesquioxane, *J. Am. Chem. Soc.,* **82**, 6194–6195 (1960).
(41) I. Hasegawa, Silicate species formed by dissolution of (2-hydroxyethyl)-trimethyl-ammonium silicate in water and in methanol, *ZEOLITE,* **12**, 720–723 (1992).
(42) Y. Haruvy and S.E. Webber, Supported sol-gel thin-film glass embodying laser dyes, 3. Optically clear SiO_2 glass thin films prepared by the fast sol-gel method, *Chem. Mater.* **4**, 89–94 (1992).
(43) L. Esquivias, C. Barrera-Solano, N. la Rosa-Fox, F.L. Cumbrera and J. Zarzycki, Determination of the skeletal density of silica gels from wide-angle X-ray diffraction, in "Ultrastructure Processing of Advanced Materials", eds. D.R. Uhlman and D.R. Ulrich, John Wiley and Sons, New York, pp. 315–325 (1992).
(44) R. Manaila and M. Zaharescu, Medium range order in high surface area amorphous silicas, *J. Mater. Sci.,* **25**, 2095–2099 (1990).
(45) B. Himmel, Th. Gerber and H. Burger, X-ray diffraction investigation of silica gel structures, *J. Non-Crystalline Solids,* **91**, 122–136 (1987).
(46) B. Himmel, Th. Gerber and H. Burger, WAXS and SAXS-investigation of structure formation in alcoholic SiO_2 solution, *J. Non-Crystalline Solids,* **119**, 1–13 (1990).
(47) K. Yamana, M. Tokonami and A. Nakano, RDF structure investigation of densified silica glasses, *J. Ceram. Soc., Japan,* **98**, 311–315 (1990).
(48) C.J. Brinker and R.A. Assink, Spinnability of silica sols; Structural and rheological criteria, *J. Non-*

Crystalline Solids, **111**, 48–54 (1989).
(49) V. Belot, R.J.P. Corriu, A.M. Flank, D. Leclercq, P.H. Mutin and A. Vioux, Thermal decomposition of hydrosilsesquioxane gels under argon, in "Euro gel '91" eds. S. Vilminot, R. Nass and H. Schmidt, Elsevier Science Publishers, B.V. pp. 77–84 (1992).
(50) K. Kamiya, S. Sakka and M. Mizutani, Preparation of silica glass fibers and transparent silica glass from silicon tetraethoxide (in Japanese), *Yogyo-Kyokai-Shi*, **86**, 553–559 (1978).